

No Very Large Scale Structure in an Open Universe¹ALBERT STEBBINS[♠] and R.R. CALDWELL^{♠♠}[♠] NASA/Fermilab Astrophysics Center, FNAL, Box 500, Batavia, Illinois 60510, USA^{♠♠} University of Cambridge, D.A.M.T.P. Silver Street, Cambridge, England, CB3 9EW

ABSTRACT. We study the effects of negative spatial curvature on the statistics of inhomogeneities in open cosmological models. In particular we examine the suppression of large-separation correlations in density and gravitational potential fluctuations and the resulting suppression of large-angle correlations in the anisotropy of the microwave background radiation. We obtain an expression which gives the *minimum* amount of suppression of correlations for any statistical distribution described by a "power spectrum". This minimum suppression requires that the correlations fall off exponentially above the curvature scale. To the extent that the observed correlations in the temperature anisotropy extend to large angular scales, one can set a lower bound to the radius of curvature and hence on Ω_0 .

1. Introduction

In this paper we examine the effects of negative spatial curvature on the statistics of inhomogeneities and in particular the microwave background radiation (MBR) anisotropy. Throughout this work, we shall consider only a cosmology described by a homogeneous, isotropic Friedmann-Robertson-Walker (FRW) spacetime with negative spatial curvature. The spatial geometry is that of H^3 , a 3-hyperboloid. We may call such an expanding spacetime "open" because the spatial manifold, H^3 , is non-compact.

In an open FRW spacetime the spatial sections are intrinsically curved with a fixed curvature radius R_{curve} at all points in space at a given time, such that the spatial Ricci scalar is ${}^3R = 6/R_{\text{curve}}^2$. On length scales much smaller than the radius of curvature, $l \ll R_{\text{curve}}$, the space effectively has a flat, Euclidean geometry. On length scales $l \gtrsim R_{\text{curve}}$, the space has a hyperbolic, Lobachevskiiian geometry. Hence, the effects of spatial curvature ought to be manifest in physical processes on length scales comparable to the radius of curvature.

Neither classical tests for curvature such as number counts and the redshift-distance relation, nor more modern techniques such as the statistics of gravitational lenses or anisotropy of clustering in redshift space, have yet to provide any conclusive evidence for or against the presence of spatial curvature [1]. Each of these tests attempts to probe the geometry directly, or indirectly through the effect of spatial curvature on the expansion of the universe. Here we examine a different consequence of the curvature, namely how the curvature influences the correlations of the inhomogeneities.

In particular we shall show that for any spectrum of inhomogeneities that correlations of the inhomogeneities must fall off exponentially for spatial separations greater than the radius of curvature in an open cosmology (see ref [2] for another discussion of these effects). Such a fall-off

¹DAMTP preprint R94/46, (Submitted to THE PHYSICAL REVIEW D)

is also possible in a flat or closed cosmology, subject to the specific behavior of the spectrum of fluctuations. Thus one cannot determine the curvature scale without making further assumptions about the spectrum of inhomogeneities [3,4,5]. Nevertheless, we may set a lower bound on the radius of curvature through this technique.

The plan of the paper is as follows. In §2 we discuss the relationship between correlation lengths of functions and the wavenumbers which parameterize the integral transforms of the functions. In §3 we show that for open cosmological models in which the inhomogeneities are described by a power spectrum there is necessarily, *on average*, a suppression of very-large-scale correlations in the inhomogeneity. Here “very-large” means larger than the curvature scale. It is shown in §4 how the suppression of large-scale power may be used to set a lower limit on the curvature scale from observations of MBR anisotropies. In §5 we examine a toy model of inhomogeneities with very-large-scale spatial structure but small-scale angular structure in the observed MBR anisotropies.

While open cosmologies have been studied by many authors the basic mathematical formulae used to describe functions in open cosmologies are probably unfamiliar to many readers. We neither wish to inundate the reader with many formulae nor to leave many of the basic mathematical results as references in other work. Therefore we present the necessary analytic tools in an appendix.

2. Patch Size, Wavenumbers, and Correlation Lengths

In this section we shall briefly discuss the relation between the correlation length of a function on the hyperboloid and the wavenumbers which characterize the mode decomposition. Unlike the flat cosmology, in an open cosmology there is a built-in spatial scale, namely the curvature scale R_{curv} . One consequence of this curvature scale is that we cannot automatically use our Euclidean intuition, which should apply to lengths below R_{curv} , to extrapolate to lengths comparable to and larger than the curvature scale.

Functions on a Euclidean space

Consider a function in 3-dimensional Euclidean space, $f(\mathbf{x})$, which consists of a positive “patch” of size L and which falls off rapidly outside of this patch. An example of this would be a top-hat function: $f(\mathbf{x}) = \Theta(L - |\mathbf{x}|)$, or a 3-dimensional Gaussian: $f(\mathbf{x}) = \exp(-|\mathbf{x}|^2/(2L^2))$. One could Fourier transform such a function

$$\tilde{f}(\mathbf{k}) = \frac{1}{(2\pi)^{\frac{3}{2}}} \int d^3\mathbf{x} f(\mathbf{x}) e^{-i\mathbf{k}\cdot\mathbf{x}}, \quad (2.1)$$

obtain the power spectrum by integrating the unit vector $\hat{\mathbf{n}}$ over the unit sphere

$$\mathcal{P}_f(k) = \frac{1}{4\pi} \int d^2\hat{\mathbf{n}} |\tilde{f}(k\hat{\mathbf{n}})|^2, \quad (2.2)$$

and obtain the 2-point correlation function

$$\Xi_f(d) = 4\pi \int_0^\infty dk k^2 \frac{\sin kd}{kd} \mathcal{P}_f(k). \quad (2.3)$$

For either of the above functions which describe a patch of size L , we see that most of the power, i.e. the dominant contribution to the integral

$$4\pi \int_0^\infty dk k^2 \mathcal{P}_f(k) = \int d^3x |f(\mathbf{x})|^2, \quad (2.4)$$

is due to values of the wavenumber $k \sim 1/L$. As well, the correlation function, $\Xi_f(d)$, is roughly constant until $d \gtrsim L$ where it starts to fall-off rapidly. Thus, the Fourier-transform coefficients at wavenumber $k \sim 1/L$ may be said to characterize the patch size and correlation length.

Functions on a hyperboloid

Now let us consider a similar function which consists of a “patch” of size L on a 3-dimensional hyperboloid. A square-integrable function on a hyperboloid, such as this patch, may be decomposed into scalar harmonics on the hyperboloid, using a Mehler-Fock transform [see eqs (A17-28)]. Certainly, these harmonics are different from the usual Fourier transform harmonics. For instance, the eigenvalues, $-k^2$, of the Laplace-Beltrami operator acting on the scalar harmonic eigenfunctions have a spectrum extending only to the range $(-\infty, -1/R_{\text{curv}}^2]$ [see eq (A17)]. If we identify k as a wavenumber, then there are no “very long wavelength” (eigen-)modes, i.e. with $k < 1/R_{\text{curv}}$. As well, one can verify that eigenfunctions with eigenvalue $-k^2$ really do vary with a typical length-scale given by k^{-1} . Hence, no eigenfunctions are smooth over a length scale much larger than the curvature radius. Thus if one has a function with a very large patch size, $L \gg R_{\text{curv}}$, one cannot guess, as we do in Euclidean space, that it is composed mostly of eigenmodes with $k \sim 1/L$, since there are no such modes. Rather, the way to compose a function with a large patch size $L \gg R_{\text{curv}}$ out of eigenfunctions which vary on length scales up to R_{curv} is to carefully add eigenfunctions with nearly the same patch size together but with opposite signs. With the right choice of coefficients one can, by delicate cancellation, construct a function with an arbitrarily large patch size.

To illustrate this we consider two examples of functions with very large patch size and their Mehler-Fock transform. It is convenient and conventional to write the Mehler-Fock transform in terms of the variable $\nu \equiv \sqrt{k^2 R_{\text{curv}}^2 - 1}$ rather than the physical wavenumber k . The range of ν is $[0, \infty)$. One should remember that $\nu = 0$ corresponds to a finite physical wavenumber $k = 1/R_{\text{curv}}$ and not to an infinitely long wavelength.

Decomposition of a radial step function on the hyperboloid

Consider first a radial step function, i.e. a top-hat:

$$f(\chi, \theta, \phi) = \Theta(\chi - \chi_0), \quad (2.5)$$

where χ is the radial coordinate measured in units of the curvature radius, θ the polar angle, and ϕ the azimuthal angle [see eq (A1)]. Since this function is spherically symmetric about the origin the transform only contains the $(l, m) = (0, 0)$ term. The Mehler-Fock transform of this function is

$$\tilde{f}_{lm}(\nu) = \frac{\sqrt{8}}{1 + \nu^2} (\cosh \chi_0 \sin \nu \chi_0 - \nu \sinh \chi_0 \cos \nu \chi_0) \delta_{l0} \delta_{m0}. \quad (2.6)$$

If the patch size, $\chi_0 R_{\text{curv}}$, is much smaller than R_{curv} , i.e. if $\chi_0 \ll 1$, then

$$\lim_{\chi_0 \rightarrow 0} \tilde{f}_{lm}(\nu) = \frac{\sqrt{8}}{\nu^2} (\sin \nu \chi_0 - \nu \chi_0 \cos \nu \chi_0) \delta_{l0} \delta_{m0} \quad (2.7)$$

which is the usual transform of a top-hat in terms of spherical Bessel functions j_l . In this case most of the power is concentrated at $\nu\chi_0 \sim 1$ or $kL \sim 1$, just as our Euclidean intuition tells us. On the other hand, if the patch size is much larger than the curvature radius, i.e. $\chi_0 \gg 1$, then the transform of eq (2.6) becomes oscillatory at $\nu \ll 1$, i.e. $kR_{\text{curv}} = 1$. Now our Euclidean intuition tells us that for $\chi_0 \gg 1$ the dominant contribution to the transform should be due to that harmonic which oscillates only on very large wavelengths. This Euclidean intuition is misleading when applied to the large-scale properties of functions on this negatively-curved space. Examine the behavior of eq (2.6) for $\chi_0 \gg 1$, varying ν . We see that the transform is dominated by contributions from a continuous range of harmonics with $0 < \nu \lesssim 1$. Thus, a single harmonic cannot identify or characterize this step function on length scales larger than the horizon radius. There is, however, nothing mysterious about the behavior of these Mehler-Fock transforms. The decomposition of this square integrable function which is constant on length scales larger than the curvature radius requires an assembly of many harmonics.

Decomposition of a Gaussian function on the hyperboloid

As a second illustration of the properties of functions and transforms on this negatively curved space, consider a Gaussian function centered at the origin:

$$f(\chi, \theta, \phi) = \exp\left(-\frac{1}{2}\frac{\chi^2}{\chi_0^2}\right). \quad (2.8)$$

The Mehler-Fock transform is

$$\tilde{f}_{lm}(\nu) = 2\sqrt{\pi}\chi_0 \sin \nu\chi_0^2 \exp\left(-\frac{1}{2}(\nu^2 - 1)\chi_0^2\right) \delta_{l0}\delta_{m0}. \quad (2.9)$$

This function $\tilde{f}_{lm}(\nu)$ is oscillatory in ν with angular frequency χ_0^2 . If $\chi_0 \ll 1$ then the amplitude of the transform is exponentially damped as $\exp(-\nu^2\chi_0^2/2)$ before the first oscillation in ν . In this case the transform closely approximates the flat-space Fourier transform. If the width of the Gaussian is much larger than the curvature radius, $\chi_0 \gg 1$, then the function oscillates many times before it is exponentially damped.

The power spectrum of the Gaussian is simply related to square of the Mehler-Fock transform of eq (2.9) via eq (A30). Note that the power spectrum of the Gaussian will also be oscillatory. One may determine which wavenumber contributes most of the power by considering the cumulative power as a function of the physical wavenumber, k , i.e.

$$\mathcal{P}_f^<(\nu) \equiv 4\pi \int_0^\nu d\bar{\nu} \bar{\nu}^2 \mathcal{P}_f(\bar{\nu}) \quad (2.10)$$

which for the Gaussian is given by

$$\mathcal{P}_f^<(\nu) = \pi\sqrt{\pi}\chi_0 \left(e^{\chi_0^2} \text{erf}\chi_0\nu - \frac{1}{2}(\text{erf}(\nu+i)\chi_0 + \text{erf}(\nu-i)\chi_0) \right). \quad (2.11)$$

We plot the shape of this function versus k for various values of χ_0 in figure 1. We see that for a Gaussian with width much smaller than R_{curv} , i.e. $\chi_0 \ll 1$, that most of the power is concentrated

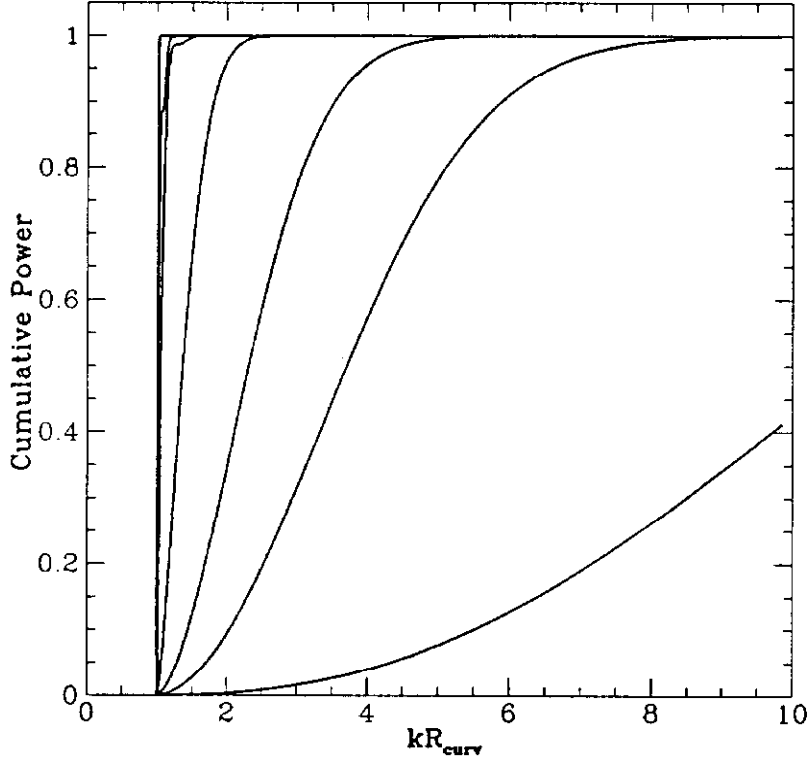


Figure 1: For a 3-d Gaussian function in hyperbolic space these curves give the cumulative power in modes with wavenumbers less than k as a function of k . From bottom to top, the displayed curves have values of the Gaussian width given by $\chi_0 = 0.1, 0.3, 0.5, 1, 2, 3, 10$. The Gaussians have been normalized to give unit total power. Observe that if the Gaussian width is much less than the curvature radius, i.e. $\chi_0 \ll 1$, that most of the power comes from $k \sim 1/(\chi_0 R_{\text{curv}})$, while if $\chi_0 \gg 1$ the power comes predominantly from k very close to $1/R_{\text{curv}}$.

at $k \sim 1/(\chi_0 R_{\text{curv}})$, i.e. wavenumbers corresponding to the width of the Gaussian. However for Gaussians with width much greater than R_{curv} the power becomes concentrated at k 's very close to the minimum value: $k = 1/R_{\text{curv}}$, which is a wavenumber much greater than $1/(\chi_0 R_{\text{curv}})$. As we shall see this smaller length scale is also reflected in the correlation function.

The notion that the Gaussian may be nearly constant on distances larger than the curvature radius does not necessarily mean that the correlations in the Gaussian extend, on average, over distances larger than the curvature scale. To see this let us first calculate the correlation function of this Gaussian as defined in (A29). We obtain

$$\Xi_f(d) = \frac{\pi^2 \chi_0^2 e^{\chi_0^2}}{2 \sinh d} \left[2 \operatorname{erf} \frac{d}{2\chi_0} - \operatorname{erf} \frac{d - 2\chi_0^2}{2\chi_0} - \operatorname{erf} \frac{d + 2\chi_0^2}{2\chi_0} \right]. \quad (2.12)$$

which is illustrated in figure 2. If $\chi_0 \ll 1$ then this correlation function falls off for $d \gtrsim \chi_0$, while for $\chi_0 \gtrsim 1$ the correlation function falls off for $d \gtrsim 1$ no matter how large is χ_0 .

How can a function have a correlation length much smaller than the size of the region over which the function extends? To understand this one should recall that Ξ_f gives the volume-weighted product of f 's at all pairs of points separated by a given distance. If the function has

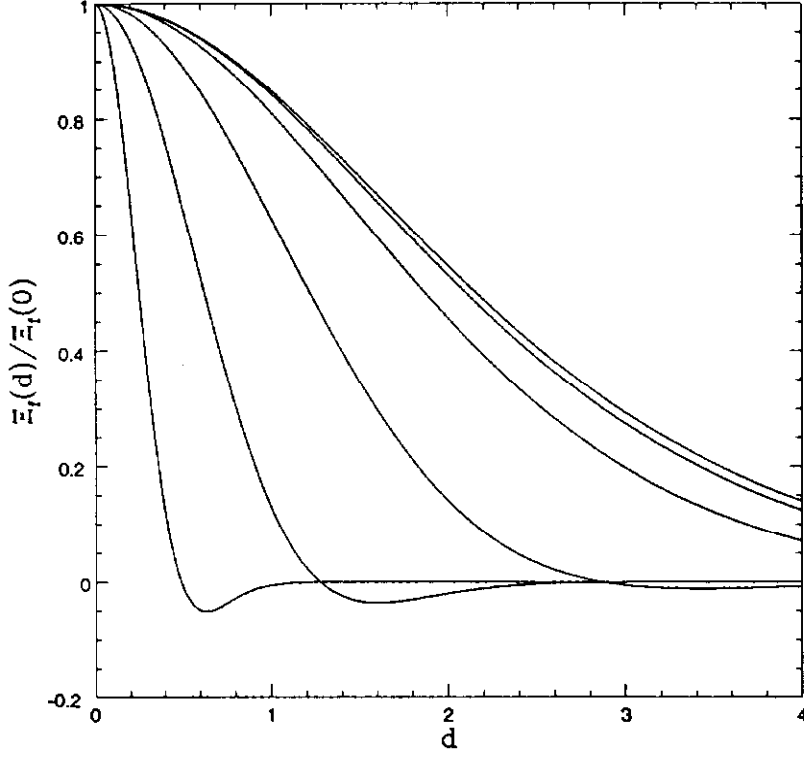


Figure 2: The ratio of the correlation function of a Gaussian at spatial separation d to the zero-lag correlation function is displayed as a function of d . From left to right, the displayed curves have values of $\chi_0 = 0.2, 0.5, 1, 2, 5, 10$ for the width of the Gaussian. Observe that even for a Gaussian with width much greater than the curvature radius, i.e. $\chi_0 \gg 1$, that the correlation function drops off rapidly for $d \gtrsim 1$. Thus, the correlation length for such a Gaussian is never much greater than the radius of curvature no matter how “wide” the Gaussian may be.

support on length scales larger than the radius of curvature, $\chi_0 \gg 1$, then this weighted product is dominated by contributions from the outer edges of the function where f falls off rapidly, i.e. it is dominated by $\chi \sim \chi_0$. The rapid variation on the outer edges overwhelms the contribution of $\chi < \chi_0$ due to the exponentially increasing volume at large radii in a hyperbolic space. Thus the correlation length of the 2-point function reflects the rapid variation at the edges of the function f and not the slower variation in the center.

3. Inequalities for Correlation Functions

In this section we shall quantify the claim that large scale correlations are suppressed in an open universe. Consider two different moments of the power spectrum of some scalar function Φ

$$M_i = 4\pi \int_0^\infty d\nu \nu^2 K_i(\nu) \mathcal{P}_\Phi(\nu) \quad (3.1)$$

for $i = 1, 2$. Here $\mathcal{P}_\Phi(\nu)$ is defined by eq (A30), and $K_i(\nu)$ is some arbitrary function of ν . We know that $\mathcal{P}_\Phi(\nu) \geq 0$, so that we have the inequalities

$$\frac{|M_2|}{M_1} \leq \max_\nu \frac{|K_2(\nu)|}{K_1(\nu)} \quad \text{if} \quad K_1(\nu) > 0 \quad (\text{Case A}) \quad (3.2)$$

or

$$\min_{\nu} \frac{K_2(\nu)}{K_1(\nu)} \leq \frac{M_2}{M_1} \leq \max_{\nu} \frac{K_2(\nu)}{K_1(\nu)} \quad \text{if} \quad K_2(\nu), K_1(\nu) > 0 \quad (\text{Case B}). \quad (3.3)$$

Now, any sort of variance or 2-point function is a moment of the power spectrum of the form of eq (3.1). From eq (A29) we see that the weighting of the power spectrum for the $\Xi_{\Phi}(d)$ is $\sin(\nu d)/(\nu \sinh d)$. For $d = 0$ this is just unity, which is positive definite. Thus the ratio of any other moment of the power spectrum to $\Xi_{\Phi}(0)$ must obey the Case A inequality. For example the ratio of the 2-point correlation at separation d to that at zero lag must obey

$$\frac{|\Xi_{\Phi}(d)|}{\Xi_{\Phi}(0)} \leq \max_{\nu} \frac{|\sin \nu d|}{\nu \sinh d} = \frac{d}{\sinh d} \quad (3.4)$$

where the maximal ratio of the weighting function occurs at $\nu = 0$. We see that the correlation function must fall off faster than $\sinh d/d$ which itself falls off like $\exp(-d)$ for $d \gtrsim 1$.

This quantifies the claim that for *any* square-integrable function, the correlation length cannot greatly exceed the curvature radius. For non-square-integrable functions the correlation function $\Xi_{\Phi}(d)$ is not defined so one must come up with a different definition of the correlation function in order to obtain the correlation length.

The functions which describe inhomogeneities in an open cosmology are typically not square-integrable. Instead they are drawn from statistically homogeneous and isotropic distributions. The expectation of bilinear moments of these functions is given by the power spectrum of eq (A32). Thus, the inequality of eq (3.4) applies equally well to the case of homogeneous random noise in an open universe, i.e. with Ξ_{Φ} replaced by ξ_{Φ} . In the case of cosmological inhomogeneities the correlation function of scalar functions must fall off exponentially beyond the curvature scale. This can be compared to flat-space where the relevant inequality is $|\xi_{\Phi}(d)| \leq \xi_{\Phi}(0)$ which is trivially satisfied for any distribution. This inequality does not imply that there cannot be large regions, much bigger than the curvature radius, in which a function is nearly constant. Rather it just says that on average - when averaging over many realizations from a homogeneous, isotropic distribution - the field may vary significantly over distances greater than the curvature radius.

The bound on the ratio of the correlation functions, eq (3.4), indicates that there is no way of smoothing functions in a statistically homogeneous way in order to increase the correlation length beyond the curvature scale. For example, one way of smoothing a function in a homogeneous and isotropic way is to convolve the function with a spherically symmetric "smoothing kernel". As indicated by eq (A35), convolution just multiplies the power spectrum by a factor and this factor drops out in the ratios which give the inequalities of eqs (3.2-3). Therefore eq (3.4) applies to the smoothed function as well as the unsmoothed function.

The reason that smoothing is unable to increase the correlation length is fairly easy to understand. The smoothing kernel must be square integrable in order for the smoothed function to retain a finite variance: $\xi_{W*\Phi}(0) < \infty$. As noted above square-integrability means that the smoothing kernel, W , must fall off exponentially at some finite distance from its "center". Due to the exponential increase in volume at large distances, it is this rapidly varying part of the kernel which will contribute most to the variation of the smoothed function. Thus the smoothing kernel cannot effectively smooth things on scales greater than the curvature radius.

4. Limits on Ω

We have shown that the correlation function of scalar quantities which describe the inhomogeneities in an open universe must fall off rapidly with large spatial separation. Can we use this property of the correlation function to set limits on the curvature radius of our own universe and thus place limits on Ω_0 ? Recall that we have only placed upper limits on the correlation function and that this upper limit becomes smaller as one decreases the radius of curvature, and therefore Ω_0 . One can therefore only hope to place a lower limit on Ω_0 from the inequality we have derived. If the correlation function starts to fall off exponentially on some scale, it could be that one has reached the curvature radius, or it could be for some other reason. However if we do not see an exponential fall-off then we have not reached the curvature scale.

We are proposing a *model independent* upper limit which only depends on the assumption of isotropy and homogeneity. If one had further knowledge of the origin of the inhomogeneities which, say, fixed the power spectrum as a function of Ω_0 then one could hope to measure Ω_0 directly from the correlation function. Of course the predicted correlation in any such model must obey the inequalities derived above. So far in this paper we have not assumed any model.

One should also recall that the correlation functions we are dealing with are expectation values under a distribution. In most cases, i.e. for ergodic processes, they should also give the correlation function for averages over the entire space. They do not give an indication of the distribution of any quantity in a finite volume, i.e. how probable it is to obtain a set of measurements. This is determined by the statistics of the random process generating the inhomogeneity. Until one makes assumptions about this distribution one cannot set any rigorous statistical limit on Ω_0 . Nevertheless if Ω_0 is sufficiently small and our observations are of a sufficiently large volume we may hope to have very good statistics. This is because, as we have demonstrated, the correlation length is limited to the curvature radius and under a large class of statistical distributions this would mean that roughly each volume of curvature radius is nearly statistically independent. Thus in our observational volume we would have a large number of independent samples of the distribution and thus a representative sample of our universe.

The obvious application of the limit on the correlation function is to the distribution of galaxies. There are, however, at least three reasons why this is not likely to be interesting. First, as we see from equation (A14) the actual size of the curvature radius is quite large, corresponding to redshifts greater than 1.7 and distances larger than $3000h^{-1}\text{Mpc}$. This is a distance much larger than it is practical to survey in the foreseeable future, as galaxies at this distance are very faint. Furthermore one would have to understand the evolution of the luminosity function of galaxies before one would be able to disentangle the evolution from the inhomogeneity. Second, it is well known that the galaxy correlation function decreases rapidly with separation as far as is measured, up to about $100h^{-1}\text{Mpc}$ which is clearly less than the curvature radius. While it is true that a simple extrapolation of this fall-off would not match the exponential fall-off required in an open universe, one would still have to measure the correlations where they were extremely small in order to put an interesting limit on Ω_0 . To do this one would have to keep systematic errors to an extremely low level. One might also think that such a measurement would be nearly impossible because of "shot noise", the statistical fluctuations caused by the finite number of galaxies. This need not be the case since the shot noise, which after all is also statistically homogeneous, would also be cutoff exponentially at the curvature radius. This decrease in shot noise is a result of the extremely large number of pairs of galaxies at large separations due to the exponentially growing

volume element in a hyperbolic space. This points to the third problem with measuring Ω_0 with galaxy correlations. Namely that if one were able to measure the galaxy distribution deep enough to notice the fall-off in correlations, one would almost certainly notice the exponentially growing volume element just by counting the number of galaxies. This classical number counting technique is almost certainly a better probe of Ω_0 than the correlation function.

To get to large enough distances one might examine the correlations in the locations of QSO's or their absorption systems. These objects are much easier to observe at large distances than galaxies, but they also suffer from having an unknown evolution of their numbers and luminosity with redshift. The number density of observed QSO's is much less than that of galaxies so it is more difficult to measure correlations on any scale, requiring a greater sample volume for a significant result. The number of Ly- α absorption systems is quite large, especially at large redshifts, but one is limited to seeing these systems only along the line-of-sight to QSO's. In neither case is the correlation function at separations of $\gtrsim 3000h^{-1}\text{Mpc}$ likely to be obtained in the near future. A simple extrapolation of correlations on smaller scales would suggest that the amplitude of inhomogeneity on these scales would be very small and difficult to measure.

An easier way to get to very large separations is to look at the MBR with which we can see back to the last-scattering epoch at a redshift $Z_{ls} \sim 10 - 1000$. Recently significant correlations in MBR temperature anisotropies have been measured using the COBE satellite [6]. Such large angle measurements are already sampling scales much larger than the curvature radius even for moderately small Ω_0 . The suppression of spatial correlations at large separations should have the greatest effect on these large angular-scale MBR measurements such as COBE. We shall now proceed to study how angular correlations of the MBR temperature anisotropies are effected by curvature. Placing the observer at the origin ($\chi = 0$) and assuming small scalar deviations from homogeneity, the MBR anisotropy on large angular scales is given by

$$\frac{\Delta T}{T}(\theta, \phi) = \frac{1}{4}\delta_\gamma(\eta_{\text{obs}} - \eta_s, \theta, \phi, \eta_s) + \Phi(\eta_{\text{obs}} - \eta_s, \theta, \phi) + 2 \int d\eta \dot{\Phi}(\eta_{\text{obs}} - \eta, \theta, \phi, \eta) - v_\chi(\eta_{\text{obs}} - \eta_s, \theta, \phi) \quad (4.1)$$

where δ_γ gives the fractional change in the photon density and Φ gives the fluctuation in the Newtonian potential, $\dot{\Phi}$ is its derivative with respect to η , and v_χ is the radially directed velocity of the photons. The quantity $\eta_{\text{obs}} - \eta_s$ gives the conformal distance to the surface of last scattering, and hence the χ coordinate of the points on the surface of last scattering.

Let us now consider the relative importance of the terms contributing to the MBR anisotropy in equation (4.1). In standard flat cosmology the Newtonian potential is constant in time so the 3rd, "integrated Sachs-Wolfe", term in equation (4.1) is very small. We also ignore the 4th, "Doppler", term in equation (4.1) which is not likely to be important on very large angular scales. It is the 1st, "density", and 2nd, "potential" terms which are most important on large scales. Whichever term dominates depends on the nature of the perturbations. For non-adiabatic fluctuations, deviations in the photon-to-baryon ratio will *usually* lead to photon density fluctuations which dominate the potential fluctuations. For adiabatic fluctuations the density fluctuations nearly cancel the potential fluctuations leading to a net anisotropy of only $\frac{1}{3}\Phi$. However in an open universe the gravitational potential will decay and the integrated Sachs-Wolfe effect will become important. Below we show that if Ω_0 is small, the large-scale correlations in the density and potential anisotropies are strongly suppressed, while the integrated Sachs-Wolfe anisotropies are less strongly suppressed. For this reason we can expect that for small Ω_0 that the large-scale anisotropies will be dominated by the integrated Sachs-Wolfe effect.

We will not consider tensor and vector fields in this work, considering only the cosmological perturbations described by scalar quantities. Whereas it is certain that scalar quantities such as density and gravitational potential fluctuations play a significant role in the observed MBR anisotropy, the relative importance of tensor and vector fields is empirically rather uncertain, and can vary greatly between different cosmological models of structure formation. We expect that the techniques used in this paper may be applied to vector and tensor modes and that one would obtain similar limits on Ω_0 from such calculations.

One might also expect the suppression of large-angle correlations of the polarization of the MBR. Polarization provides certain advantages over temperature anisotropies in obtaining limits on Ω_0 . Firstly because the MBR polarization, generated by electron-photon scattering, is confined to the surface of last scattering, while MBR anisotropy may be generated at smaller redshifts via the integrated Sachs-Wolfe effect. We will see below that the integrated Sachs-Wolfe anisotropies yield much less stringent limits on Ω_0 than those generated on the surface of last scattering. Secondly there is no need to subtract off the monopole or dipole components of polarization, they are zero. Such subtractions in the case of anisotropies lead to “artificial” correlations at large angular separations. Of course the main disadvantage of MBR polarization is that it has not yet been detected. Furthermore it is likely to be at a much smaller amplitude than temperature anisotropies, and thus more difficult to measure accurately. We will not consider MBR polarization further in this paper.

Anisotropies from the Surface of Last Scattering

Let us first consider the MBR anisotropies generated at the surface-of-last-scattering, i.e. by ignoring the integrated Sachs-Wolfe contribution. Thus we consider the density and potential contributions to the anisotropy of equation (4.1). The 2-point angular correlation function of this component of the anisotropy can be easily written in terms of, $\xi_{\frac{1}{4}\delta+\Phi}$, the spatial 2-point correlation function of the scalar field $\frac{1}{4}\delta + \Phi$ or its power spectrum, $P_{\frac{1}{4}\delta+\Phi}$, i.e.

$$C_{ls}(\psi) = \xi_{\frac{1}{4}\delta+\Phi}(d(\eta_{obs} - \eta_s, \eta_{obs} - \eta_s, \psi)) = 4\pi \int d\nu \nu P_{\frac{1}{4}\delta+\Phi}(\nu) \frac{\sin \nu d(\eta_{obs} - \eta_s, \eta_{obs} - \eta_s, \psi)}{\sinh d(\eta_{obs} - \eta_s, \eta_{obs} - \eta_s, \psi)} \quad (4.2)$$

where ψ is the angular separation and $d(\chi_1, \chi_2, \psi)$ defined in equation (A3) gives the comoving distance between the two points on the surface of last scattering an angle ψ apart. As computed in the previous section, the inequality of equation (3.4) when applied to the intrinsic anisotropy gives

$$\frac{|C_{ls}(\psi)|}{C_{ls}(0)} \leq \frac{d(\eta_{obs} - \eta_s, \eta_{obs} - \eta_s, \psi)}{\sinh d(\eta_{obs} - \eta_s, \eta_{obs} - \eta_s, \psi)}. \quad (4.3)$$

Using equation (A13) to calculate $\eta_{obs} - \eta_s$ as a function of Ω_0 we have plotted the upper limit of equation (4.3) in figure 3 for various values of Ω_0 . We see that the required fall-off in the correlation function is very striking even for moderately small Ω_0 .

One cannot compare the curves of figure 3 directly to $C(\psi)$ of the MBR anisotropy observed by COBE primarily because MBR anisotropy experiments do not measure the intrinsic anisotropy on the surface of last scattering but rather the sum of this with many other effects. Furthermore MBR anisotropy experiments such as COBE do not measure the 2-point function of the anisotropy on the sky. Instead the anisotropy is convolved with the beam pattern of the experiment. The

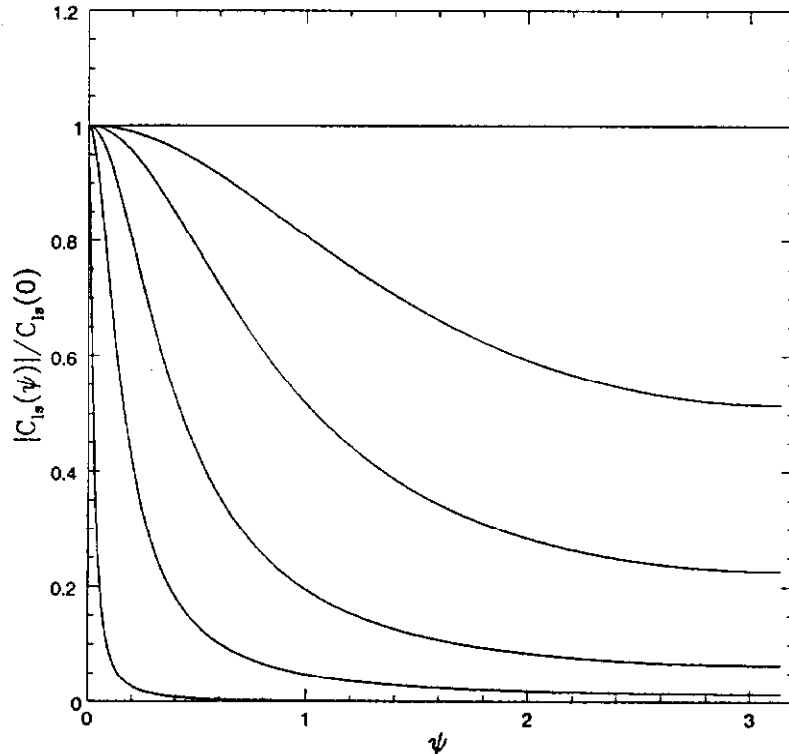


Figure 3: For anisotropies produced on the surface-of-last-scattering, this curve gives the upper bound on the ratio of the absolute value of the correlation function at angular separation ψ to the zero-lag correlation, as a function of ψ and for various values of Ω_0 . From top to bottom the curves are for $\Omega_0 = 1, 0.75, 0.5, 0.25, 0.1, 0.01$. The redshift of last scattering used in these figures is $z_{ls} = 1000$. Note that the required fall-off in the correlation function is very striking even for moderately small Ω_0 .

beam patterns are not sensitive at all to the monopole component of the anisotropy pattern and the dipole component of the anisotropy pattern is explicitly subtracted. We have seen above that the limit of equation (3.4) is equally valid before and after 3-dimensional convolution in a hyperbolic space. However convolutions on the sky, which are intrinsically anisotropic, will invalidate this formula. Nevertheless we can use the inequalities of equation (3.2-3) to come up with alternative inequalities which apply to the convolved anisotropy with monopole and dipole subtraction.

Effects of Beam Smearing

Here we demonstrate the effects of Gaussian convolution in an attempt to address the problem of fluctuations on the surface of last scattering more realistically. We convolve the anisotropy pattern on the sky with a Gaussian window function of the form

$$f(\psi; \sigma) = \frac{\exp \frac{\cos \psi}{\sigma^2}}{4\pi\sigma^2 \sinh \frac{1}{\sigma^2}} \quad (4.4)$$

where the width of the Gaussian may also be written in terms of its FWHM, θ_{FWHM} , given by

$$\sigma = \sqrt{\frac{1 - \cos \frac{1}{2}\theta_{\text{FWHM}}}{\ln 2}} \quad (4.5)$$

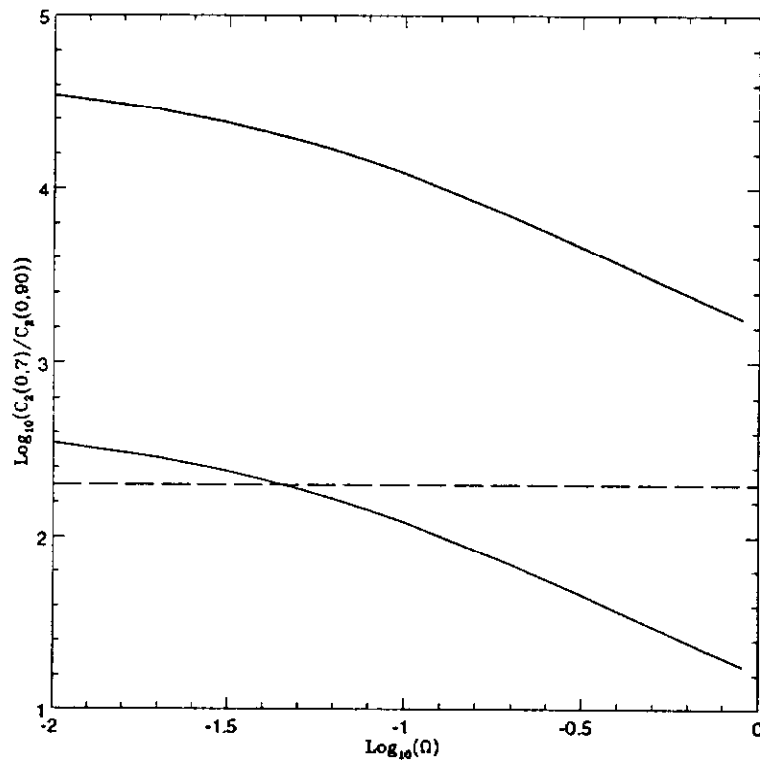


Figure 4: The upper and lower bounds on the logarithm of the ratio of the zero-lag correlation function smoothed by a Gaussian of widths 7 and 90 degrees, as a function of Ω_0 is displayed. For comparison, the central value of ratio obtained from the COBE 2-year data is displayed as a horizontal line. If the anisotropies were completely generated on the surface of last-scattering and there were no sampling or instrumental errors on this COBE result then one would conclude that $\Omega_0 \gtrsim 0.05$.

Applying this smoothing function to the anisotropy pattern, we find the smoothed correlation function is

$$C_{ls}(\psi; \sigma) = \frac{1}{16} \int d\nu |\delta_{rms}(\nu)|^2 \left(\sigma^2 \sinh \frac{1}{\sigma^2} \right)^{-2} \sum_{J=0}^{\infty} \frac{2J+1}{4\pi} |\Pi_{\nu}^J(\eta_{obs} - \eta_s) i_J(\frac{1}{\sigma^2})|^2 P_J(\cos \psi). \quad (4.6)$$

Here, $i_J(x) = i^J j_J(ix)$, is a modified spherical Bessel function and $P_J(x)$ a Legendre polynomial. Due to the simple form of the Gaussian smoothing function, we may easily subtract the contributions of any multipole moment of the anisotropy pattern by eliminating that term from the sum over J . We shall adopt the notation $C_{ls}(\psi; \sigma)_l$ to indicate that the sum over J begins with the $J = l$ term.

Consider the zero-lag correlation function:

$$C_{ls}(0; \sigma)_l = \frac{1}{16} \int d\nu |\delta_{rms}(\nu)|^2 \left(\sigma^2 \sinh \frac{1}{\sigma^2} \right)^{-2} \sum_{J=l}^{\infty} \frac{2J+1}{4\pi} |\Pi_{\nu}^J(\eta_{obs} - \eta_s) i_J(\frac{1}{\sigma^2})|^2. \quad (4.7)$$

Comparing equation (3.1) with (4.7), we see that the term in the above equation which corresponds to $K(\nu, z)$ is positive for any smoothing width σ . Therefore, as in equation (3.3), we may place an

upper and lower bound on the ratio of two variances with different smoothing widths. In particular

$$\min_{\nu} r(\sigma_1, \sigma_2, \nu)_l \leq \frac{C_{ls}(0; \sigma_1)_l}{C_{ls}(0; \sigma_2)_l} \leq \max_{\nu} r(\sigma_1, \sigma_2, \nu)_l \quad (4.8)$$

where the ratio, $r(\sigma_1, \sigma_2, \nu)_l$, is given by

$$r(\sigma_1, \sigma_2, \nu)_l = \left[\frac{\sigma_2^2 \sinh \frac{1}{\sigma_2^2}}{\sigma_1^2 \sinh \frac{1}{\sigma_1^2}} \right]^2 \frac{\sum_{J=l}^{\infty} (2J+1) |\Pi_{\nu}^J(\eta_{\text{obs}} - \eta_{ls}) i_J(\frac{1}{\sigma_1^2})|^2}{\sum_{J=l}^{\infty} (2J+1) |\Pi_{\nu}^J(\eta_{\text{obs}} - \eta_{ls}) i_J(\frac{1}{\sigma_2^2})|^2}. \quad (4.9)$$

The minimum and maximum values of $r(\sigma_1, \sigma_2, \nu)_l$ may be easily computed numerically.

In figure 4 we present the upper and lower bounds on the ratio of MBR variance with 7° and 90° smoothing, having subtracted the monopole and dipole moments. We have computed the same ratio $C_{ls}(0; \sigma(7^\circ))_2 / C_{ls}(0; \sigma(90^\circ))_2$ from the 2-year results of the COBE DMR experiment [6]. Comparing the observed results with predicted bounds, we see that Ω_0 , the present-day cosmological density parameter, is only weakly restricted.

Adiabatic Fluctuations and the MBR

The above models of anisotropy were not completely realistic since the integrated Sachs-Wolfe effect was ignored. The relative importance of the integrated Sachs-Wolfe effect depends somewhat on the nature of the perturbations. Here we shall consider adiabatic fluctuations including the density, potential, and integrated Sachs-Wolfe contributions to the anisotropies. Following ref [4] and assuming an adiabatic growing mode in a dust-dominated open universe we find that the MBR anisotropy is given by

$$\frac{\Delta T}{T}(\theta, \phi) = \frac{1}{3} \Phi(\eta_{\text{obs}}, \theta, \phi) + 2 \int_0^{\eta_{\text{obs}}} d\eta \Phi_0(\eta_{\text{obs}} - \eta, \theta, \phi) F'(\eta) \quad (4.10)$$

where the time evolution of the potential is given by the function F (see equation (A16)). The angular correlation function may thus be written as

$$\begin{aligned} C_{\text{ad}}(\psi) = & \frac{1}{9} \xi_{\Phi}(d(\eta_{\text{obs}}, \eta_{\text{obs}}, \psi)) + \frac{2}{9} \int_0^{\eta_{\text{obs}}} d\eta F'(\eta) \xi_{\Phi}(d(\eta_{\text{obs}}, \eta_{\text{obs}} - \eta, \psi)) \\ & + 4 \int_0^{\eta_{\text{obs}}} d\eta_1 F'(\eta_1) \int_0^{\eta_{\text{obs}}} d\eta_2 F'(\eta_2) \xi_{\Phi}(d(\eta_{\text{obs}} - \eta_1, \eta_{\text{obs}} - \eta_2, \psi)) \end{aligned} \quad (4.11)$$

or

$$C_{\text{ad}}(\psi) = 4\pi \int_0^{\infty} d\nu \nu \mathcal{P}_{\Phi}(\nu) K_{\text{ad}}(\nu, \psi). \quad (4.12)$$

Here the kernel is

$$\begin{aligned} K_{\text{ad}}(\nu, \psi) = & \frac{1}{9} \frac{\sin \nu d(\eta_{\text{obs}}, \eta_{\text{obs}}, \psi)}{\nu \sinh d(\eta_{\text{obs}}, \eta_{\text{obs}}, \psi)} \\ & + \frac{2}{3} \int_0^{\eta_{\text{obs}}} d\eta F'(\eta) \frac{\sin \nu d(\eta_{\text{obs}}, \eta_{\text{obs}} - \eta, \psi)}{\nu \sinh d(\eta_{\text{obs}}, \eta_{\text{obs}} - \eta, \psi)} \\ & + 4 \int_0^{\eta_{\text{obs}}} d\eta_1 F'(\eta_1) \int_0^{\eta_{\text{obs}}} d\eta_2 F'(\eta_2) \frac{\sin \nu d(\eta_{\text{obs}} - \eta_1, \eta_{\text{obs}} - \eta_2, \psi)}{\nu \sinh d(\eta_{\text{obs}} - \eta_1, \eta_{\text{obs}} - \eta_2, \psi)} \end{aligned} \quad (4.13)$$

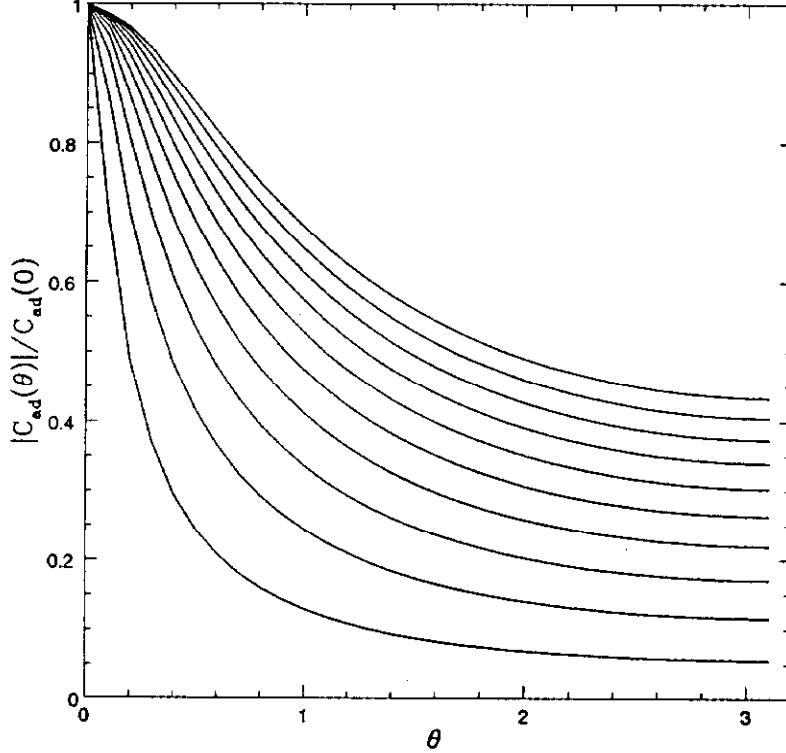


Figure 5: As in figure 3 except that this bound is for purely adiabatic fluctuations and the curves, from top to bottom, are for Ω_0 decreasing from 0.1 to 0.01 in units of 0.01. Observe that the required fall-off in the correlation function is less striking than in figure 3 even for small values of Ω_0 .

which at zero lag is

$$K_{\text{ad}}(\nu, 0) = \frac{1}{9} + \frac{2}{3} \int_0^{\eta_{\text{obs}}} d\eta F'(\eta) \frac{\sin \nu \eta}{\nu \sinh \eta} + 4 \int_0^{\eta_{\text{obs}}} d\eta_1 F'(\eta_1) \int_0^{\eta_{\text{obs}}} d\eta_2 F'(\eta_2) \frac{\sin \nu(\eta_2 - \eta_1)}{\nu \sinh(\eta_2 - \eta_1)}. \quad (4.14)$$

To find the maximum allowed values of $C_{\text{ad}}(\psi)/C_{\text{ad}}(0)$ we should maximize the ratio of the integrands $K_{\text{ad}}(\nu, \psi)/K_{\text{ad}}(\nu, 0)$ with respect to ν . This has been done numerically and the results are displayed in figure 5 for Ω_0 in the range $[0.01, 0.1]$. Much smaller values of Ω_0 are required to produce the same suppressions exhibited in figure 3, and therefore the limits on Ω_0 for adiabatic perturbations will be much less stringent than found in the case where the anisotropies are generated solely on the surface of last scattering.

The reason that the bound on Ω_0 using $C_{\text{ad}}(\psi)/C_{\text{ad}}(0)$ is weaker than the bound obtained using $C_{\text{ls}}(\psi)/C_{\text{ls}}(0)$ is not hard to understand. All of the contributions to $C_{\text{ls}}(\psi)$ are at the relatively large comoving distance $\eta_{\text{obs}} - \eta_{\text{s}}$, which for even moderately low values of Ω_0 is much larger than a curvature radius away. Unless the angular separation, ψ , is very small two points on the sky will be several curvature radii away from each other. In this case $d \gtrsim 1$ so that correlations will be suppressed exponentially. However for the integrated Sachs-Wolfe effect the anisotropies are generated at much closer distances to the observer. In fact one needs $\Omega_0 \lesssim 0.1$ before most of the integrated Sachs-Wolfe anisotropy is generated at more than a curvature radii away. Thus for a given angular separation, ψ , the anisotropies along different lines of sight are generated at relatively small spatial separations and the $d/\sinh d$ suppression of spatial correlations is smaller.

Thus for adiabatic fluctuations the suppression of correlations at a given angular scale is reduced because one is sampling a much smaller spatial separation than for anisotropies generated on the surface-of-last-scattering.

One should also notice that in all cases the upper bound on the angular correlation function stops decreasing rapidly at some moderate angle. This can be understood in terms of the peculiar geometrical property of hyperbolic spaces. Namely that the spatial separation of two points an angle ψ apart as seen from an observer will have only a weak dependence on the angle if the distance from the observer is much larger than R_{curv} (see equation (A4)). Thus the $d/\sinh d$ suppression of spatial correlations saturates at some moderate angular scale and does not cause much further suppression at larger angular separations.

5. Anisotropies Without Power Spectra or Square-Integrable Functions

So far we have considered global perturbations which are described by a power spectrum or local perturbations described by square-integrable functions. We have shown that for such perturbations, the correlations necessarily fall off at the curvature radius. For homogeneous Gaussian random noise in terms of the usual basis functions, this behavior leads to functions with support on length scales which are never much bigger than the curvature radius. It is certainly feasible to construct functions with a patch size much larger than the curvature radius, although these functions would not be very likely to arise from Gaussian random noise. As long as such functions are square-integrable the correlation function will still fall off rapidly at the curvature radius. This is due to the fact that the “edges” of the regions of positive or negative support, which must vary rapidly in order to insure that the function is square-integrable, dominate the average. Thus, we are lead to the question of whether there exist non-square-integrable functions which have correlation lengths much larger than the curvature radius and whether these are relevant to cosmology [7].

In this section, we shall examine two non-square-integrable functions with a correlation length which is much larger than the curvature radius. We shall consider two examples of such a function, and show that if these functions represent MBR temperature as emitted from the surface-of-last-scattering, that the resultant anisotropy is still suppressed on large angular scales if the surface-of-last-scattering is much further from the observer than the curvature radius. As we shall see the amount of suppression need not be as large as we have found so far.

A Step Function Along the Central Plane

Consider a function which takes one value in one half of the space and the opposite value in the other half. In particular consider the function

$$T(\chi, \theta, \phi) = \text{sgn}\left(\frac{\pi}{2} - \theta\right) \quad (5.1)$$

This clearly splits the space H^3 in half since there is a reflection symmetry about $\theta = \frac{\pi}{2}$. One might argue that this function is just the limiting form of a very large top-hat function centered at infinity, which is square-integrable, and therefore should also have rapidly falling correlations on average. For any pair of points with separation r , however, there are infinitely more pairs for which both points lie to one side of the plane than pairs which straddle the plane. Therefore, one would also sensibly argue that the 2-point correlation function is really just +1, independent

of separation. (A simpler example of such a function is just a constant function, whose 2-point correlation function is independent of separation. This clearly violates the limits which apply to functions described by a power spectrum. We have chosen not to consider such a function, since it involves no inhomogeneity.)

We shall consider the scenario in which equation (5.1), through some process, determines the temperature of photons as they are emitted at the time of last-scattering. That is, the temperature of the photons observed on the celestial sphere will take one of two values, $+1$ for those photons emitted at points with $\theta < \frac{\pi}{2}$ and -1 for the rest. The boundary between these two temperatures is given by the intersection of the sphere of radius η_{obs} centered on the observer and the plane $\theta = \frac{\pi}{2}$. An observer located within a distance η_{obs} of the plane will see a disk-like temperature anisotropy in the shape of a circle while an observer located further than a distance η_{obs} of the plane will see no temperature inhomogeneity on the sky. Now we will determine the distribution of the sizes of disks as seen by observers.

We would like to determine the measure for the distribution of disk sizes as seen by observers along the plane. Let us begin by defining the distance from an observer to the central plane, D_c , to be the shortest distance connecting the observer to any point on the central plane. For an observer located at coordinates (χ, θ, ϕ) ,

$$D_c = \cosh^{-1}(\sqrt{1 + \sinh^2 \chi \cos^2 \theta}) \quad (5.2)$$

gives the distance to the central plane.

The disk size is just a function of the distance of the observer from the central plane, D_c . Therefore it suffices to determine the distribution of D_c . We would like to determine the volume-weighted average of D_c . Unfortunately this is not completely well defined since the volume of points with D_c in some interval is infinite. To better define how to weight the different distances one can make use of the fact that there is an isometry corresponding to translations along the plane. Combining these translations with reflections about the central plane we may find that all points a given distance D_c from the central plane are isometric. By requiring that the weighting scheme have the same symmetries unambiguously determines the distribution of D_c . To determine this distribution, consider the translations in the “ x ” and “ y ” directions, generated by the two Killing vectors which map the central plane into itself (see equation A10)

$$\begin{aligned} \xi_i^x &= (\cos \phi \sin \theta, \sinh \chi \cosh \chi \cos \theta \cos \phi, -\sinh \chi \cosh \chi \sin \theta \sin \phi) \\ \xi_j^y &= (\sin \phi \sin \theta, \sinh \chi \cosh \chi \cos \theta \sin \phi, \sinh \chi \cosh \chi \sin \theta \cos \phi) \end{aligned} \quad (5.3)$$

The proper invariant weight, $w(D_c)$ is given by the requirement that

$$\xi_{[i}^x \xi_{j]}^y D_{c,k] = w(D_c) \epsilon_{ijk} \quad (5.4)$$

where $[ijk]$ indicates antisymmetrization and ϵ_{ijk} is the completely anti-symmetric symbol, such that $\epsilon_{123} = \sqrt{\gamma}$. This is equivalent to requiring the volume swept out by an infinitesimal translation in the two directions and by an infinitesimal change in D_c satisfy

$$\dot{w}(D_c) \propto \frac{\delta V}{\delta \lambda_x \delta \lambda_y \delta D_c}. \quad (5.5)$$

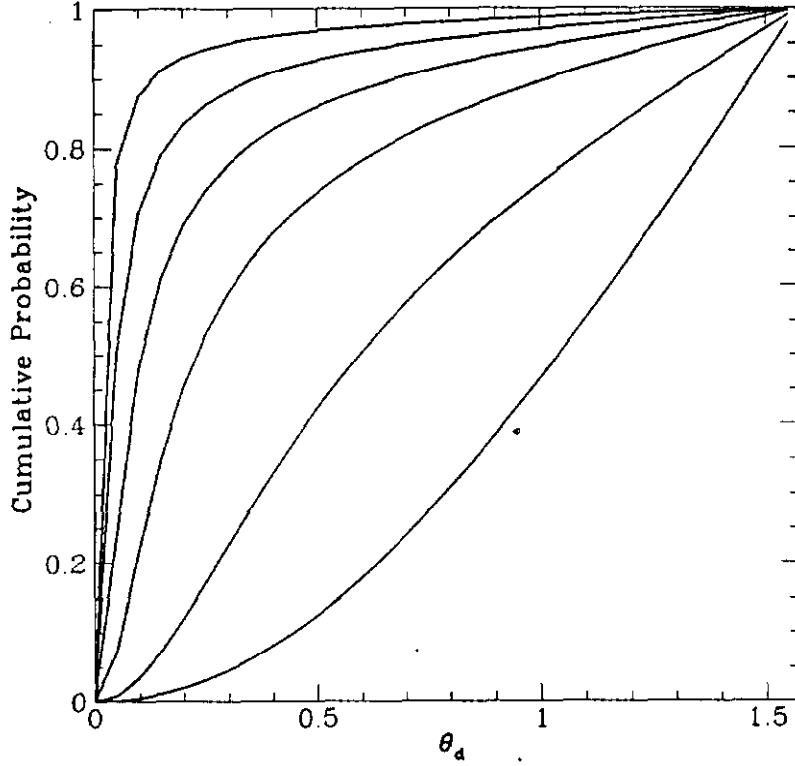


Figure 6: In a universe where half of spacetime is one temperature and half another, this curve gives the probability of observing a hot or cold circular disc on the sky of angular radius θ_d or smaller. From bottom to top the curves correspond to $\Omega_0 = 0.99, 0.5, 0.2, 0.1, 0.05, 0.02$ in a dust dominated universe, or a horizon size $\eta_{\text{obs}} = 0.20, 1.8, 2.9, 3.6, 4.4, 5.3$ times the curvature radius. Note that if $\Omega_0 \ll 1$ most observers who observe hot/cold spots will observe spots with very small angular size.

Along the $\theta = 0$ axis, we find that $w(D_c) = \frac{1}{6} \cosh^2 D_c$. Interpreting this weight as a probability distribution we find

$$p(D_c) dD_c \propto \cosh^2 D_c dD_c. \quad (5.6)$$

This measure is not normalizable, but since we are only interested in the range of values $D_c < \eta_{\text{obs}}$, we can still obtain sensible results. The cumulative probability that D_c is less than some value is

$$P_<(D_c) \propto 2D_c + \sinh 2D_c. \quad (5.7)$$

For an observer a distance D_c away from the plane the angular radius θ_d subtended by the disk of different temperature is given by

$$\theta_d = \cosh^{-1}(\tanh D_c \coth \eta_{\text{obs}}). \quad (5.8)$$

So we find that the cumulative probability that θ_d is larger than some value is

$$P_>(\theta_d) \propto 2 \tanh^{-1}(\cos \theta \tanh \eta_{\text{obs}}) + \sinh 2 \tanh^{-1}(\cos \theta \tanh \eta_{\text{obs}}), \quad (5.9)$$

and the distribution function is

$$p(\theta_d) = \frac{dP_>(\theta_d)}{d\theta_d} \propto \frac{4}{2\eta_{\text{obs}} + \sinh 2\eta_{\text{obs}}} \frac{\sin \theta_d \tanh \eta_{\text{obs}}}{(1 - \cos^2 \theta_d \tanh^2 \eta_{\text{obs}})^2}. \quad (5.10)$$

Here we have chosen the normalization so that the integral from 0 to $\frac{\pi}{2}$ is unity. If $\eta_{\text{obs}} \gg 1$ then this distribution is strongly peaked near $\theta \rightarrow 0$, i.e. very small disk sizes.

In figure 6, we have plotted the probability of observing a patch of angular size θ_d , for values of $\eta_{\text{obs}} = \frac{1}{2}R_{\text{curv}}, R_{\text{curv}}, 2R_{\text{curv}}$. The peak in the distribution shifts to small angular patch sizes with increasing η_{obs} , according to the formula $\theta_{\text{peak}} = \min[\arcsin(1/(\sqrt{3} \sinh \eta_{\text{obs}})), \pi/2]$. For a dust-dominated expansion, relating η_{obs} to the surface of last scattering at a redshift of $Z_{\text{ls}} = 1000$, the three curves in figure 6 correspond to values of the cosmological density parameter $\Omega_0 = 0.9, 0.8, 0.4$ respectively. Thus, we find that for a cosmological model in which temperature anisotropy is determined by the non-integrable function with correlation length longer than the radius of curvature, given by eq (5.1), then the spatial curvature *still* serves to suppress the angular size of disks of temperature inhomogeneities on the celestial sphere. As well, in such a toy model, observation of a large disk of temperature inhomogeneity on the celestial sphere may be translated into a lower bound on Ω_0 , the cosmological density parameter.

A Radial Gradient

Another class of functions one might consider are those which are spherically symmetric about the origin, i.e.

$$T(\chi, \theta, \phi) = F(\chi). \quad (5.11)$$

As above we shall suppose that $T(\chi, \theta, \phi)$, through some process, determines the temperature of photons as they are emitted at the time of last-scattering. Clearly all observers will see an axisymmetric temperature pattern with the axis of symmetry being the direction from the observer to the center of symmetry. If we place the observer a distance R_{obs} from the center of symmetry and draw a sphere of radius η_{obs} centered about the observer, one finds that the distance, R , from the center of symmetry to a point on this sphere is given by (see eq (A3))

$$\cosh R(\alpha) = \cosh R_{\text{obs}} \cosh \eta_{\text{obs}} - \sinh R_{\text{obs}} \sinh \eta_{\text{obs}} \cos \alpha, \quad (5.12)$$

where α is the angle on the observers sky between the direction to this point on the sphere and the direction to the center of symmetry. All distances are measured in units of R_{curv} . Here η_{obs} approximates the distance to the surface-of-last-scattering so the temperature pattern is given by

$$\frac{\Delta T}{T}(\alpha) = F(R(\alpha)), \quad (5.13)$$

If T is not square-integrable then it is difficult to define an average over observers in order to conclude whether the anisotropies more often come from large or small angular scales. However any sensible average would give much weight to observers very far from the center, and one can show that for observers sufficiently far from the center the anisotropy pattern becomes independent of this distance. This is illustrated by the relationship

$$R(\alpha) - R_{\text{obs}} \approx \ln |\cosh \eta_{\text{obs}} - \sinh \eta_{\text{obs}} \cos \alpha| \quad R_{\text{obs}} \gg 1, \eta_{\text{obs}}, \quad (5.14)$$

One would think that to make large angle anisotropies one should take $F(R)$ to be slowly varying. If we take $F(R)$ to be sufficiently slowly varying that a 1st order Taylor series is a good approximation in the interval $R \in [R_{\text{obs}} - \eta_{\text{obs}}, R_{\text{obs}} + \eta_{\text{obs}}]$, then

$$\frac{\Delta T}{T}(\alpha) - \overline{\frac{\Delta T}{T}} = F'(R_{\text{obs}}) \left(\ln |\cosh \eta_{\text{obs}} - \sinh \eta_{\text{obs}} \cos \alpha| + 1 - \eta_{\text{obs}} \frac{\cosh \eta_{\text{obs}}}{\sinh \eta_{\text{obs}}} \right). \quad (5.15)$$

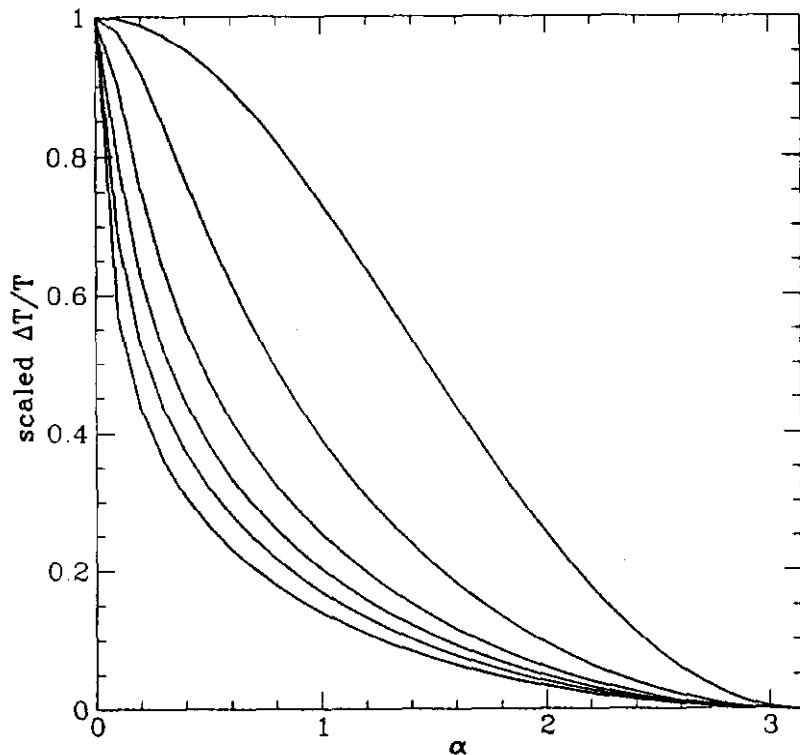


Figure 7: For a universe with a spatial temperature distribution which is spherically symmetric and which has a large spatial coherence we plot the shape of the temperature pattern which would be observed far from the center of symmetry. The temperature depends only on α , the angle from the direction toward the center of symmetry, and has been scaled so that the temperatures go from 0 to 1. From top to bottom the curves correspond to $\Omega_0 = 0.99, 0.5, 0.2, 0.1, 0.05, 0.02$ in a dust dominated universe, or a horizon size $\eta_{\text{obs}} = 0.20, 1.8, 2.9, 3.6, 4.4, 5.3$ times the curvature radius. Note that as Ω decreases the pattern becomes a smaller and smaller spot in the direction toward the center of symmetry.

Here we have explicitly subtracted the mean temperature averaged over the sky since this contributes isotropy not anisotropy. In figure 7 we plot this temperature pattern for various values of η_{obs} . Again we find that as we increase η_{obs} past the curvature radius that the temperature anisotropy becomes more and more concentrated on smaller angular scales.

According to eq (4.3) and figure 3 all square-integrable functions will have a correlation function that will approach a δ -function at zero lag in the limit $\eta_{\text{obs}} \gg 1$. We will now show that if F is not square-integrable then this limiting form may be evaded. In the limit that η_{obs} becomes very large, but still much smaller than the coherence length of F , we obtain the limiting form of eq (5.15)

$$\frac{\Delta T}{T}(\alpha) - \overline{\frac{\Delta T}{T}} = F'(R_{\text{obs}}) \left(\ln \left| \frac{1 - \cos \alpha}{2} \right| + 1 \right) \quad R_{\text{obs}} \gg \eta_{\text{obs}} \gg 1. \quad (5.16)$$

This exhibits a divergent hot or cold spot at $\alpha = 0$, but note that the spot is only logarithmically divergent. If $0 < \Omega_0 \ll 1$ and $F(R_{\text{obs}})$ was some power law at large R_{obs} then the observers at large distance from the origin would see a pattern like that described by eq (5.16). Note that such a power law would ensure that F was not square-integrable and thus might evade the limits set in §4. Since essentially all the volume is at large distance one could reasonably claim that the shape

of the volume averaged angular correlation function for the anisotropy is just given by the shape of the angular correlation function of the pattern described by eq (5.16). Since the logarithm is an integrable singularity it is clear that $C_{ls}(\theta; 0)_1$ is finite at $\theta = 0$ and most other values of θ . Thus if F is asymptotically a power law then the correlation function does not obey the limit of eq (4.3).

In this section we have examined two spatial temperature distributions with very large scale spatial coherence. In both cases the anisotropy patterns that they induce are increasingly small angular scales as one increases the radius of the surface-of-last-scattering past the curvature radius, i.e. as one decreases Ω_0 well below unity. This illustrates that there is no simple correspondence between large spatial coherence and large angular coherence in an open universe. It is not clear whether there are any temperature configurations in which most observers would see only dipole (and/or quadrupole) temperature anisotropy patterns if Ω_0 is very small. This is in contrast to Euclidean space where it is quite easy to push most of the anisotropies to the lowest multipoles by putting most of the inhomogeneity on super-horizon scales. In the case of radial gradients it was shown that only a finite fraction of the anisotropy is pushed to large multipole moments as Ω_0 is decreased. Thus it is possible for the large angle correlations to remain large even if Ω_0 is small. A question we have not fully answered is whether this is ever likely to occur in a cosmological setting. Clearly this will never occur in any distribution described by a power spectrum.

While we have considered only anisotropies generated on the surface-of-last-scattering in this section we would expect qualitatively similar results for anisotropies generated by adiabatic fluctuations. One would have to go to significantly larger values of η_{obs} in order to obtain the same level of large-angle suppression for adiabatic inhomogeneities.

6. Conclusion

In this work we have examined certain statistical properties of functions in a hyperbolic space, with applications to density fluctuations and MBR anisotropies in an open universe. We have shown that large-scale correlations are exponentially suppressed for separations above the curvature scale in an open universe. This suppression is generic to the open cosmology, rather than being a feature of a particular model of inhomogeneities in an open cosmology. We have further shown how the observed presence of large angular scale anisotropy may be used to give a lower bound on the cosmological density parameter Ω_0 which is independent of the shape of the spectrum of perturbations. We have done this by considering two generic mechanisms for the generation of MBR anisotropy, i.e. adiabatic or last-scattering-surface fluctuations, although we expect that similar sorts of limits may be obtained for any combination primordial adiabatic and isocurvature fluctuations.

The best limits on Ω_0 come from the largest angular scale anisotropies, such as measured by COBE [6]. We have not made a detailed comparison of the suppression of large-scale anisotropies due to curvature with the COBE data. Effects such as instrumental noise and cosmic variance have not been considered and we have not tried to find the most stringent limit on Ω_0 by searching for an optimal statistic. Furthermore any formal limit would require assumptions about the “statistics” of the anisotropies. The comparison with COBE in figure 4 does indicate that even with extremely optimistic assumptions only a relatively weak lower limit, $\Omega_0 \gtrsim 0.05$ can be obtained. Considering adiabatic fluctuations while including instrumental noise and a reasonable model for cosmic variance would yield a significantly less stringent limit. It seems likely that the lower limit on Ω_0 from statistics of anisotropies will never yield a more stringent limit than is obtained from other

methods. Limits from statistics are, however, a qualitatively different types of model-independent limit than others that have been used.

We have illustrated the suppression of large-scale correlations with two classes of functions, namely square-integrable functions, and homogeneous and isotropic ensembles of functions described by a power spectrum in the usual way. The former provides an instructive example while the latter might describe the inhomogeneities in our own universe. These two types of functions were chosen for a very practical reason, namely that for these functions we know how to compute averages to obtain 2-point correlation functions: a volume average for the former and an ensemble average for the latter. It has suggested by K. Gorski [7] that there may be distributions of cosmological inhomogeneities which cannot be described by a power spectrum in the usual way, and that such a distribution may not exhibit the suppression of large-scale correlations found here. This has yet to be shown.

In §5 we have considered spatial distributions which are not square-integrable and unlike anything one is likely to find from a homogeneous distribution of functions. These functions can be said to have very large spatial coherence, although this is difficult to quantify since the 2-point correlation function as normally defined would not be finite. Nevertheless, in spite of this large coherence we find that if these functions represented temperatures that the typical anisotropies, i.e. for most observers, would have significant power on very small angular scales if $\Omega_0 \ll 1$. It is the geometry of the hyperbolic space that causes large spatial correlations lengths to result in small angular correlation lengths for these configurations. For the configurations examined in §6 we find that the suppression of large-angle anisotropies when Ω_0 is small can be much less than the suppression which is required for spatial distributions of temperatures describes by a power spectrum. It is therefore possible to find spatial distributions where the volume-averaged anisotropy has large angular coherence when Ω_0 is small. Whether such distributions are ever likely to arise in any model of statistically homogeneous random noise is an unanswered question. In any model described by a power spectrum such configurations would essentially never occur.

Acknowledgements: Thanks to Bruce Allen, Martin Bucher, Josh Frieman, Kris Gorski, David Lyth, Adi Nusser, Misao Sasaki, and Igor Tkachev for useful discussions. The work of AS and RRC is supported by the NASA through grant number NAG-5-2788 (at Fermilab). The work of RRC is funded by PPARC through grant number GR/H71550 (at Cambridge).

Appendix: Tools for an open universe

Coordinates in an open universe

The line element for a homogeneous, isotropic FRW spacetime with spatial geometry of H^3 , a 3-hyperboloid, is

$$ds^2 = a^2(\eta) (-d\eta^2 + d\chi^2 + \sinh^2 \chi (d\theta^2 + \sin^2 \theta d\phi^2)) \quad (\text{A1})$$

where a is the expansion scale factor, $\eta \in (0, \infty)$ is the conformal time, and the spatial coordinates χ , which gives the comoving radius from the central point, θ which is the polar angle from an axis, and ϕ which is an azimuthal angle about this axis, have ranges $[0, \infty)$, $[0, \pi]$, and $[0, 2\pi]$, respectively. Of course the choice of the central point and the polar axis is arbitrary. Units of length are carried by the expansion scale factor. The spatial, (χ, θ, ϕ) , part of this metric we refer to as γ_{ij} and its determinant as γ . The curvature of the spatial sections is $-1/a^2$ in physical units, which decrease with time. This means that in units of comoving curvature radius, R_{curv}/a is unity. The volume element of a spatial section is given by

$$dV = a^3 \sinh^2 \chi \sin \theta d\chi d\theta d\phi, \quad (\text{A2})$$

so that the volume within a distance χ grows like $\sim e^{2\chi}$ for χ larger than the curvature scale, $\chi \gg 1$. The comoving geodesic distance, $d(\chi_1, \chi_2, \psi)$ between two points, $(\chi_1, \theta_1, \phi_1)$ and $(\chi_2, \theta_2, \phi_2)$ is given by

$$\begin{aligned} \cosh d &= \cosh \chi_1 \cosh \chi_2 - \sinh \chi_1 \sinh \chi_2 \cos \psi \\ \cos \psi &= \cos \theta_1 \cos \theta_2 + \sin \theta_1 \sin \theta_2 \cos(\phi_1 - \phi_2) \end{aligned} \quad (\text{A3})$$

Here ψ is the angle between the direction to the two points as seen from the origin. Equation (A3) is simply the law of cosines for a hyperbolic geometry. One curious property is that if the distance from the origin is much greater than the curvature scale, then

$$\cosh d \approx \exp(\chi_1 + \chi_2 + \ln[\sin^2(\psi/2)]) \quad \chi_1, \chi_2 \gg 1. \quad (\text{A4})$$

Hence, if the surface of last-scattering of MBR photons is much further from us than the curvature radius then most pairs of points on this surface are approximately at the same distance from each other with only a weak, logarithmic, dependence on the angle between them.

Isometries

Here we may list the isometries of the 3-hyperboloid. The group of isometries of H^3 is $O(1, 3)$, which has 6 generators. The isometries of the 3-hyperboloid may be specified by the 6 linearly independent Killing vector fields on the manifold, i.e. vector fields satisfying Killing's equation

$$\xi_{(a)}^{i;j} + \xi_{(a)}^{j;i} = 0 \quad a = 1, \dots, 6. \quad (\text{A5})$$

The Killing vectors generate diffeomorphisms of $H^3 \rightarrow H^3$ of the form

$$x^i \rightarrow X_{(a)}^i(\{x^j\}, \lambda) \quad (\text{A6})$$

where $X_{(a)}^i(x, \lambda)$ is a solution of the 1st order ordinary differential equation

$$\frac{d}{d\lambda} X_{(a)}^i = \xi_{(a)}^i \quad (\text{A7})$$

with initial conditions

$$X_{(a)}^i(\{x^j\}, 0) = x^i. \quad (\text{A8})$$

Linear combinations of the diffeomorphisms may be constructed to form a (sub-)group of isometries of the space. Additional discrete symmetries may lead to parts of the group which are disconnected from the identity.

The Killing vectors generating the 3 rotations, analogs to the rotations about the “x”, “y”, and “z” axes in a Euclidean space, are respectively

$$\begin{aligned} \xi_{(1)}^i &= (0, \sin \phi, \frac{\cos \theta}{\sin \theta} \cos \phi) \\ \xi_{(2)}^i &= (0, \cos \phi, -\frac{\cos \theta}{\sin \theta} \sin \phi) \\ \xi_{(3)}^i &= (0, 0, 1). \end{aligned} \quad (\text{A9})$$

These Killing vectors form the sub-group $O(3)$ with topology S^2 . The 3 “translations”

$$\begin{aligned} \xi_{(4)}^i &= (\cos \phi \sin \theta, \frac{\cosh \chi}{\sinh \chi} \cos \phi \cos \theta, -\frac{\cosh \chi \sin \phi}{\sinh \chi \sin \theta}) \\ \xi_{(5)}^i &= (\sin \phi \sin \theta, \frac{\cosh \chi}{\sinh \chi} \sin \phi \cos \theta, \frac{\cosh \chi \cos \phi}{\sinh \chi \sin \theta}) \\ \xi_{(6)}^i &= (\cos \theta, \frac{\cosh \chi}{\sinh \chi} \sin \theta, 0) \end{aligned} \quad (\text{A10})$$

are analogs to the translations of the origin along the “x”, “y”, and “z” axes in a Euclidean space.

Expansion Law

The matter in our universe appears to be dominated by cold, pressureless dust. In the absence of a cosmological constant, the cosmological density parameter is given by

$$\Omega = \frac{8\pi G\rho}{3H^2} = \frac{1}{1+a} \quad a = \frac{1-\Omega}{\Omega} \quad (\text{A11})$$

where H is the Hubble constant and the normalization of the scale factor, a , is chosen so that $a = 1$ when $\Omega = \frac{1}{2}$. The evolution of the scale factor follows as

$$a(\eta) = \sinh^2 \frac{\eta}{2}. \quad (\text{A12})$$

The horizon and the density parameter are related by

$$\eta = \ln \frac{2 - \Omega + \sqrt{(2 - \Omega)^2 - \Omega^2}}{\Omega}. \quad (\text{A13})$$

In physical units the curvature radius is given by

$$R_{\text{curv}} = \frac{c}{H\sqrt{1-\Omega}} = \frac{3000 h^{-1} \text{Mpc}}{\sqrt{1-\Omega}} \quad H = 100h \text{ km/s/Mpc.} \quad (\text{A14})$$

Even if Ω is very small we see that the curvature scale remains very large. Galaxies one curvature radius away have a redshift greater than $z \geq e - 1 \approx 1.7$ and the lower limit is only approached for very small Ω . Thus, the surface of last scattering, at a redshift $z \sim 1000$, is more than one curvature radius away for $\Omega \lesssim 0.8$. Interestingly, in the limit $\Omega \rightarrow 0$, an object located at redshift z can be at most $\ln z$ curvature radii away.

Growth of Perturbations

If the matter present in the universe is slightly inhomogeneously distributed but has negligible vorticity, and the cosmos has negligible gravity wave content then the metric of (A1) may be modified to be of the form

$$ds^2 = a^2(\eta) \left(-(1 + 2\Phi) d\eta^2 + d\chi^2 + (1 - 2\Phi) \sinh^2 \chi (d\theta^2 + \sin^2 \theta d\phi^2) \right) \quad \Phi \ll 1 \quad (\text{A15})$$

where $\Phi(\chi, \theta, \phi, \eta)$ is the Newtonian gravitational potential induced by the inhomogeneities. Again assuming the matter pressure is negligible one finds that the evolution of this potential is given by

$$\Phi(\chi, \theta, \phi, \eta) = \Phi_0(\chi, \theta, \phi) F(\eta) \quad F(\eta) = 5 \frac{\sinh^2 \eta - 3\eta \sinh \eta + 4 \cosh \eta - 4}{(\cosh \eta - 1)^3} \quad (\text{A16})$$

where the growing mode solution which is regular at $\eta = 0$ has been chosen. We may see that this function $F(\eta)$, the growth factor, is exponentially suppressed as $\eta \gg 1$.

Scalar Spherical Harmonics on H^3

We shall be interested in the harmonics which form a complete basis for square integrable functions on H^3 [3,8]. These harmonics, written as $Y_{\nu lm}(\chi, \theta, \phi)$, have the following properties. The harmonics satisfy the (Helmholtz) wave equation

$$[\gamma^{ij} \nabla_i \nabla_j + (\nu^2 + 1)] Y_{\nu lm}(\chi, \theta, \phi) = 0 \quad \nu \geq 0. \quad (\text{A17})$$

The harmonics are orthogonal:

$$\int \sqrt{\gamma} d^3 x Y_{\nu lm}(\chi, \theta, \phi) Y_{\nu' l' m'}^*(\chi, \theta, \phi) = \delta(\nu - \nu') \delta_{ll'} \delta_{mm'}. \quad (\text{A18})$$

This expression also fixes the normalization of the harmonics. These harmonics may be expressed in more familiar terms as the Helmholtz solid harmonics on the hyperboloid

$$Y_{\nu lm}(\chi, \theta, \phi) = \Pi_{\nu}^l(\chi) Y_{lm}(\theta, \phi) \quad (\text{A19})$$

where $Y_{lm}(\theta, \phi)$ is the usual spherical harmonic on S^2 , and Π_{ν}^l is the (Mehler -) Fock harmonic.

$$\Pi_{\nu}^l(\chi) = |\Gamma[i\nu + l + 1]/\Gamma[i\nu]| \sinh^{-1/2} \chi P_{i\nu-1/2}^{-(l+1/2)}(\cosh \chi) \quad (\text{A20})$$

Here $P_n^{-l}(z)$ is the Legendre function [9] of the first kind, defined for $z \geq 1$,

$$P_n^{-l}(z) \equiv \frac{1}{\Gamma(1+l)} \left(\frac{1-z}{1+z} \right)^{l/2} {}_2F_1[-n, n+1; 1+l; \frac{1-z}{2}]. \quad (\text{A21})$$

Useful relations of these functions, as well as a short history, may be found in [9,10]. To generate values of the associated Legendre functions, we may use the integral definition, valid for the values of μ and ν relevant for our work,

$$P_\nu^\mu(\cosh \chi) = \sqrt{\frac{2}{\pi}} \frac{\sinh^\mu \chi}{\Gamma(\frac{1}{2} - \mu)} \int_0^\chi dt \frac{\cosh(\nu + \frac{1}{2})t}{(\cosh \chi - \cosh t)^{\mu + \frac{1}{2}}}. \quad (\text{A22})$$

Thus we find $P_{\nu-1/2}^{-1/2}(\cosh \chi) = \sqrt{\frac{2}{\pi \sinh \chi}} \frac{\sin \nu \chi}{\nu}$. The recursion relation

$$P_{\nu+1}^\mu(z) - P_{\nu-1}^\mu(z) = (2\nu+1) \sqrt{z^2-1} P_\nu^{\mu-1}(z) \quad (\text{A23})$$

may then be used to more easily generate the functions. (Note that the definition of the associated Legendre functions $P_\nu^\mu(x)$ and $P_\nu^\mu(z)$ in Gradshteyn & Ryzhik (1980) is reversed.)

Another notation has been used in the literature to represent the Fock harmonics (Tomita 1982):

$$\Xi_l(\nu, \chi) = \sqrt{\frac{2}{\pi}} \frac{(-)^{l+1}}{\sqrt{N_l(\nu)}} \sinh^l \chi \left(\frac{d}{d \cosh \chi} \right)^{l+1} \cos(\nu \chi) \quad (\text{A24})$$

with normalization such that

$$\int_0^\infty d\chi \sinh^2 \chi \Xi_l(\nu, \chi) \Xi_l(\nu', \chi) = \delta(\nu - \nu'). \quad (\text{A25})$$

Here, $N_l(\nu) = \prod_{j=0}^l (\nu^2 + j^2)$. For integer values of l , i.e. those functions needed here, the harmonics $\Xi_l(\nu, \chi)$ are equivalent to $\Pi_\nu^l(\chi)$. However, we shall use the Fock harmonics expressed with the associated Legendre functions in this paper.

Mehler-Fock Transform

Any scalar function, $\Phi(\vec{x})$, on H^3 may be decomposed in terms of Fock harmonics so long as it is a square integrable function, i.e. the integral

$$\int \sqrt{\gamma} d^3 x |\Phi(\vec{x})|^2 \quad (\text{A26})$$

converges. For the metric given by equation (A1), this condition amounts to requiring that $|\Phi(\chi, \theta, \phi) e^{-\chi}|$ be finite as $\chi \rightarrow \infty$. If satisfied, we may express the function $\Phi(\vec{x})$ as

$$\Phi(\vec{x}) = \int d\nu \sum_{l=0}^{\infty} \sum_{m=-l}^l \tilde{\Phi}_{lm}(\nu) Y_{\nu lm}(\vec{x}). \quad (\text{A27})$$

Denoting the mode coefficients by a tilde we find

$$\tilde{\Phi}_{lm}(\nu) = \int \sqrt{\gamma} d^3 x \Phi(\vec{x}) Y_{\nu lm}^*(\vec{x}). \quad (\text{A28})$$

This is the Mehler-Fock transform, which takes the place of the Fourier transform on H^3 .

Power Spectrum and Correlation Functions for Square Integrable Functions

We shall define the correlation function of a square integrable, spherically symmetric function to be the volume weighted integral of the product of the functions evaluated at points separated by a distance d . In particular for the function $W(\vec{x})$, we define the correlation function to be

$$\begin{aligned}\Xi_W(d) &= \frac{\int \sqrt{\gamma} d^3x \int \sqrt{\gamma'} d^3x' W(\vec{x}) W(\vec{x}') \delta(d - |\vec{x} - \vec{x}'|)}{\int \sqrt{\gamma} d^3x \delta(d - |\vec{x}|)} \\ &= 4\pi \int_0^\infty d\nu \nu \mathcal{P}_W(\nu) \frac{\sin \nu d}{\sinh d}\end{aligned}\tag{A29}$$

Here we define the power spectrum as

$$\mathcal{P}_W(\nu) = \nu^{-2} \sum_{l=0}^{\infty} \sum_{m=-l}^l |\tilde{W}_{lm}(\nu)|^2 \tag{A30}$$

For a spherically symmetric function the sum is merely a formality, as the only non-zero contribution to the Fock transform, $\tilde{W}_{lm}(\nu)$, is the $(l, m) = (0, 0)$ mode coefficient.

Power Spectra

The inhomogeneities in our universe, such as the gravitational potential, Φ , may be described in terms of scalar functions. Now, the Cosmological Principle states that we expect the universe to be on average homogeneous and isotropic. Thus, we expect Φ to be determined by some homogeneous isotropic distribution. By these considerations one may determine that the expectation under this distribution of the second moment of the mode coefficients is of the form

$$\langle \tilde{\Phi}_{lm}(\nu) \tilde{\Phi}_{l'm'}^*(\nu') \rangle = (2\pi)^3 P_\Phi(\nu) \delta(\nu - \nu') \delta_{ll'} \delta_{mm'}.\tag{A31}$$

Here the function $P_\Phi(\nu)$ is the power spectrum which is given by

$$P_\Phi(\nu) = (2\pi)^{-3} \sum_{l=0}^{\infty} \sum_{m=-l}^l |\tilde{\Phi}_{lm}(\nu)|^2 \tag{A32}$$

if the distribution is ergodic. This power spectrum, $P_\Phi(\nu)$, differs from the power spectrum for square-integrable function, $\mathcal{P}_\Phi(\nu)$, defined in eq (A31). Since a statistically homogeneous function must maintain the same level of inhomogeneity in all regions of the space it will not be square-integrable. The functions $\tilde{\Phi}_{lm}(\nu)$ will not be finite but must be considered as distributions. The spectrum $P_\Phi(\nu)$, however, will remain finite or at least integrable, while for a statistically homogeneous function, Φ , \mathcal{P}_Φ would diverge. Of course, P_Φ , is non-negative but is otherwise arbitrary. In terms of the power spectrum the 2-point correlation function of Φ may be written as

$$\xi_\Phi(d) = \langle \Phi(\chi, \theta, \phi) \Phi^*(\chi', \theta', \phi') \rangle = 4\pi \int_0^\infty d\nu \nu P_\Phi(\nu) \frac{\sin \nu d}{\sinh d} \tag{A33}$$

where d is the geodesic distance between the two points (χ, θ, ϕ) and (χ', θ', ϕ') given in equation (A3).

Let us pause to examine equation (A33), which will give us some insight into the general claim made in this paper, that large scale structure is suppressed in an open universe. Observe the dependence on the separation distance d by the correlation function $\xi_{\Phi}(d)$. The integrand is suppressed exponentially for $d \gg 1$, that is, for separations larger than the curvature radius. We may recall that on a spatially flat space, the integrand of the correlation function diminishes only as the inverse of the separation distance. Thus the 2-point correlation function is exponentially suppressed at large separations in an open universe, and in some way is more strongly suppressed than in a spatially flat universe.

Convolution Theorem

If we draw functions from an isotropic, homogeneous random distribution and convolve each of these functions with a spherically symmetric window function, we obtain a new distribution of functions which is also homogeneous and isotropic. Given a function W , the convolution with Φ is

$$[W * \Phi](\chi, \theta, \phi) \equiv \int \sqrt{\gamma} d^3 x' W(d) \Phi(\chi', \theta', \phi') \quad (\text{A34})$$

where again d is the geodesic distance between the (χ, θ, ϕ) and (χ', θ', ϕ') . In terms of the transform of W , the power spectra of the convolved function is

$$P_{W*\Phi}(\nu) = (2\pi)^3 \mathcal{P}_W(\nu) P_{\Phi}(\nu) \quad (\text{A35})$$

where P_W is the power spectrum of the convolving function. If the volume integral of the convolving function is normalized to unity, then the convolution is simply a weighted average. For such an average the variance may only diminish, i.e.

$$\int \sqrt{\gamma} d^3 x W(d) = 1 \quad \text{implies} \quad (2\pi)^3 \mathcal{P}_W(\nu) \leq 1 \quad \forall \nu. \quad (\text{A36})$$

In flat space, equation (A36) would also imply $(2\pi)^3 \mathcal{P}_W(0) = 1$ so that $P_{W*\Phi}(0) = P_{\Phi}(0)$, which is just another way of saying that the mean is not effected by a convolution. However on this hyperbolic space one finds $(2\pi)^3 \mathcal{P}_W(0) \neq 1$ so that $P_{W*\Phi}(0) \neq P_{\Phi}(0)$. This is represented in the fact that the lowest, $\nu = 0$, Fock harmonic does not generally represent the mean value of the spherically symmetric function, except in the limit $R_{\text{curv}} \rightarrow \infty$. This is another reflection of the lack of large scale power in an open universe which is demonstrated in this paper.

REFERENCES

1. J. Peebles, "Principles of Physical Cosmology", Princeton University Press, Princeton, 1993, pp. 310-342.
2. M. Wilson, *Free-Streaming in Cosmological Models with Spatial Curvature*, *Astrophys. J. Lett.* **253** (1983), L53-L56.
- 3a. M. Wilson, Ph.D. thesis (1982), University of California, Berkeley.
- 3b. M. Wilson, *On the Anisotropy of the Cosmological Background Matter and Radiation Distribution. II. The Radiation Anisotropy in Models with Negative Curvature*, *Astrophys. J.* **271** (1983), 2-15.
4. M. Kamionkowski and D. Spergel, *Large-Angle Cosmic Microwave Background Anisotropies in an Open Universe*, *Astrophys. J.* **432** (1994), 7-16.
- 5a. N. Gouda, N. Sugiyama, and M. Sasaki, *Large Angle Anisotropy of the Cosmic Microwave Background in an Open Universe*, *Prog. Theor. Phys.* **85** (1990), 1023-1040.
- 5b. D. Lyth and E. Stewart, *Inflationary Density Perturbations with $\Omega < 1$* , *Phys. Lett. B* **252** (1990), 336-342.
- 5c. M. Kamionkowski, B. Ratra, D. Spergel, and N. Sugiyama, *CMB Anisotropy in an Open Inflation, CDM Cosmogony*, astro-ph/9406069, IASSNS - HEP - 94 - 39, CfPA - TH - 94 - 27 (1993).
- 5d. U. Pen and D. Spergel, *Cosmic Microwave Anisotropies from Topological Defects in an Open Universe*, astro - ph / 9408103 (1994).
- 5e. M. Bucher, A. Goldhaber, and N. Turok, *An Open Universe from Inflation*, hep-ph/9411206.
- 5f. B. Allen and R. Caldwell, *Cosmic Background Radiation Temperature Fluctuations in a Spatially-Open Inflationary Universe*, in preparation (1994).
6. C. Bennett *et al*, *Cosmic Temperature Fluctuations from Two Years of COBE-DMR Observations*, COBE preprint 94-01 (1994).
7. K. Gorski, private communications (1992).
- 8a. N. Vilenkin and Y. Smorodinskii, *Invariant Expansions of Relativistic Amplitudes*, *Soviet Physics JETP* **19** (1964), 1209-1218.
- 8b. K. Tomita, *Tensor Spherical and Pseudo-Spherical Harmonics in Four-Dimensional Spaces*, *Prog. Theor. Phys.* **68** (1982), 310-313.
9. I. Gradshteyn and I. Ryzhik, "Tables of Integrals, Series and Products", Academic Press, New York, 1980.
10. M. Zhurina and L. Karmazina, "Tables and Formulae for the Spherical Functions $P_{-1/2+i\tau}^m(z)$ ", Pergamon Press, Oxford, 1966.